



OPEN Sinularin induces autophagy-dependent cell death by activating ULK1 and enhancing FOXO3-ATG4A axis in prostate cancer cells

Xiang-yu Meng^{1,2,8}, Yi Li^{3,8}, Ze-jun Yan^{1,2,4}, Sha-zhou Ye^{1,2}, Ke-jie Wang^{1,2}, Jun-feng Chen^{1,2}, Rui Yu⁵✉ & Qi Ma^{1,6,7}✉

Sinularin is a natural product extracted from soft coral and is shown to exhibit antitumor effects against multiple human cancers. We previously showed that Sinularin induces apoptotic cell death via stabilizing the FOXO3 protein in prostate cancer cells. In this study, we demonstrated that Sinularin triggers autophagy via two different mechanisms in prostate cancer cells. First, Sinularin reduced the S757 phosphorylation of ULK1 protein, which was mediated by mTOR, leading to ULK1 activation and autophagy initiation. Second, Sinularin enhanced the expression of autophagic protein ATG4A, which is the key regulator in the formation of autophagosome, through a FOXO3-dependent transcriptional mechanism. Next, we identified that ATG4A is a new target gene of the transcription factor FOXO3. Additionally, we also found that Sinularin-induced autophagy promoted survivin degradation and led to cell apoptosis. Taken together, these findings suggest that Sinularin induces prostate cancer cell autophagy by promoting autophagy initiation through activation of ULK1 and formation of autophagosome through the FOXO3-ATG4A pathway.

Keywords Sinularin, Prostate cancer, Autophagy, Apoptosis, FOXO3

Marine natural products are potential and promising sources for drug development^{1,2}. Before 1970, two therapeutic compounds of marine origin, cytarabine (arabinosyl cytosine, ara-C) and protamine sulfate, were approved for clinical usage, followed by vidarabine (arabinosyl adenine, ara-A) in 1976^{3–5}. To date, approximately 20 drugs from marine sources are approved for clinical usage, and most of them are approved for anti-cancer therapy⁶.

Sinularin, also referred to as flexibilide, was shown to be effective in anti-multiple human cancers, including melanoma⁷, gastric⁸, oral^{9–11}, hepatocellular^{12,13}, breast^{14,15}, lung¹⁶, and kidney cancers¹⁷. Our previous study showed that Sinularin induces intrinsic cell apoptosis by stabilizing the FOXO3 protein in prostate cancer cells¹⁸. In this study, we further elucidated the mechanisms involved in Sinularin-induced prostate cancer cell death. Our results indicated that Sinularin promotes autophagy initiation by activation of ULK1, which was regulated by the mTOR pathway, and Sinularin also enhances the formation of autophagosomes through the FOXO3 pathway. We identified ATG4A as a new FOXO3 target gene. Moreover, we revealed survivin degradation via Sinularin-induced autophagy, which also leads to cell apoptosis. Taken together, these findings revealed complicated mechanisms involved in Sinularin-induced prostate cancer cell death and demonstrated that Sinularin is a potential marine nature product for further drug development in the treatment of prostate cancer.

¹Ningbo Clinical Research Center for Urological Disease, The First Affiliated Hospital of Ningbo University, #59 Liuting Street, Ningbo 315010, Zhejiang, China. ²Ningbo Top Medical and Health Research Program, The First Affiliated Hospital of Ningbo University, #59 Liuting Street, Ningbo 315010, Zhejiang, China. ³Department of Urology, The Second Affiliated Hospital, School of Medicine, Zhejiang University, #88 Jiefang Road, Hangzhou 310009, Zhejiang, China. ⁴Department of Urology, The First Affiliated Hospital of Ningbo University, #59 Liuting Street, Ningbo 315010, Zhejiang, China. ⁵Department of Biochemistry and Molecular Biology, Zhejiang Key Laboratory of Pathophysiology, Health Science Center, Ningbo University, #818 Fenghua Road, Ningbo 315211, Zhejiang, China. ⁶Comprehensive Genitourinary Cancer Center, The First Affiliated Hospital of Ningbo University, #59 Liuting Street, Ningbo 315010, Zhejiang, China. ⁷Yi-Huan Genitourinary Cancer Group, Ningbo 315010, Zhejiang, China. ⁸Xiang-yu Meng and Yi Li contributed to this work equally. ✉email: yurui@nbu.edu.cn; fyymaqi@nbu.edu.cn

siRNA name	siRNA sequence (5'-3')
siNC	UUCUCCGAACGUGUCACGU
siFOXO3 #2	GCUCACUUCGGACUCACUU
siFOXO3 #3	CCUCAUCUCCACACAGAAU
siATG4A #1	GCCUCCCGAUUCUUUAACU
siATG4A #2	GCCUGGGCAUAAACCAAAU
siATG4A #3	GCCUUGUUCAGAAGGAAAU

Table 1. The sequence of SiRNAs.

Genes	Primer sequences (5'-3')	
β-Actin	Forward	TCTCCCAAGTCCACACAGG
	Reverse	GGCACGAAGGCTCATCA
ATG4A	Forward	GGAATTGGCCAGGATGACA
	Reverse	TGCTGCTTCCTAAGATCCA

Table 2. Primers for quantitative real-time PCR.

Materials and methods

Cell culture and transfection

The cell lines used in the study 293T, LNCaP and PC-3 were purchased from the Stem Cell Bank, Chinese Academy of Sciences (Shanghai, China). The cells were cultured in the indicated media (DMEM for 293T cells, RPMI 1640 for LNCaP cells, F-12 K for PC-3 cells) (Procell, Wuhan, China) supplemented with 10% FBS (PAN, Germany). All human cell lines have been authenticated using STR (or SNP) profiling within the last three years. All experiments were performed with mycoplasma-free cells. RNAi-Mate reagent (GenePharma, Shanghai, China) was used for cell transfection following the manufacturer's instructions. The siRNA sequences are listed in Table 1.

Cell viability assay

Cell Titer 96[®] Aqueous One Solution Reagent (MTS, Promega, USA) was used to determine cell viability according to previous methods¹⁹.

Propidium iodide (PI) staining

Cultured cells were digested, harvested and washed with precooled PBS. Then, the cells were stained with PI and detected via flow cytometry.

Cell apoptosis assay

An Annexin V-FITC/PI cell apoptosis kit (MultiSciences, Hangzhou, China) was used to detect apoptosis according to previous methods¹⁷.

Transmission electron microscopy (TEM)

Cultured cells were digested and harvested, fixed with 2.5% glutaraldehyde at room temperature in the dark for 30 min, and then transferred to 4 °C for storage. A transmission electron microscopy (TEM) assay was performed using Servicebio[®] (Wuhan, China).

Antibodies and Western blot

The western blot analysis was performed as previously described²⁰. Antibodies against β-Actin (#4970), LC3A/B (#4108), SQSTM1/p62 (#5114), mTOR (#2972), p-mTOR Ser2448 (#2971), ULK1 (#8054), p-ULK1 S757 (#14202), ATG4A (#7613), Caspase-3 (#14220), PARP (#9532), FOXO3 (#2497), Survivin (#2803), Anti-rabbit IgG HRP-linked Antibody (#7074) and Anti-mouse IgG HRP-linked Antibody (#7076) were purchased from Cell Signaling Technology (USA).

RNA extraction and quantitative real-time PCR (qRT-PCR)

RNA extraction and qRT-PCR were performed according to previous methods²¹. The primer sequences are listed in Table 2.

Immunofluorescence staining

Immunofluorescence staining was used to detect LC3 according to previous methods²². Anti-LC3A/B antibody (#4108; Cell Signaling Technology, USA) and goat anti-rabbit IgG H&L (Alexa Fluor[®] 488) (ab150077; Abcam, USA) were used.

Luciferase reporter assay

We constructed a sensor vector containing the ATG4A promoter. The full-length ATG4A promoter, shorting ATG4A promoter, and mutant ATG4A promoter were cloned and inserted into a firefly luciferase reporter vector. The ATG4A promoter firefly luciferase reporter vector or control reporter vector, FOXO3 overexpression vector or control vector, and Renilla luciferase reporter vector were co-transfected into 293T cells. Luciferase activity was measured with a Dual-Luciferase Reporter Assay System (Promega, USA) according to the manufacturer's protocols.

Statistical analysis

Differences among the control and tested groups were analyzed using one-way ANOVA followed by the Dunnett post hoc test. Differences between the two groups were assessed using Student's t-test. $P < 0.05$ indicated statistical significance, and all the data are presented as the mean \pm standard deviation (SD).

Results

Inhibition of autophagy and apoptosis blocks Sinularin induced prostate cancer cell death

In the previous study, we demonstrated that Sinularin induced PUMA-dependent intrinsic cell apoptosis by stabilizing the FOXO3 protein¹⁸. However, we found that inhibition of apoptosis by pan-caspase inhibitor Z-VAD-FMK only partially reduced Sinularin induced cell death in our current study (Fig. 1A–D). These findings encouraged us to further explore the mechanisms involved in Sinularin-induced cell death. We first asked if the ferroptosis pathway is involved in Sinularin induced cell death since triggering ferroptosis is a new approach for cell death²³, however, both ferroptosis inhibitors, ferrostatin-1 (Fer-1), and deferoxamine mesylate (DFOM), had no significant effect on Sinularin induced cell death (Supplementary Fig. 1). Then we used autophagy inhibitor chloroquine (CHQ) to see if autophagy is involved in Sinularin-induced cell death, and after treatment with CHQ, Sinularin-induced cell death was dramatically reduced (Fig. 1E–H). We then treated prostate cancer cells with both Z-VAD-FMK and CHQ to inhibit both apoptosis and autophagy, and the result showed that the number of cells was restored to the normal level observed in cells without treatment of Sinularin (Fig. 1I–L). Taken together, these results indicated Sinularin induces both autophagy and apoptosis in prostate cancer cells.

Sinularin induces autophagy by activating ULK1

We then used transmission electron microscopy (TEM) to detect autophagic vacuoles in PC-3 cells treated with Sinularin for 24 h. As shown in Fig. 2A, Sinularin dramatically increased the number of autophagic vacuoles. Moreover, Sinularin treatment enhanced LC3-II processing and p62 protein degradation, two hallmarks of cell autophagy (Fig. 2B). Furthermore, we quantified the LC3-containing immunofluorescent puncta to assess the impact of Sinularin on autophagic flux in PC-3 cells. As shown in Fig. 2C, Sinularin significantly increased the number of autophagic puncta.

Next, we asked whether Sinularin induced autophagy through the pathway of mTOR, as mTOR is the key molecule involved in triggering autophagy²⁴. Indeed, Sinularin largely reduced mTOR phosphorylation and eliminated mTOR-dependent ULK1 phosphorylation at the S757 site, which is a key character for ULK1 activation²⁵ (Fig. 2D). ULK1 selective inhibitor MRT68921 largely rescued Sinularin-induced viability inhibition (Fig. 2E) and reduced autophagy in Sinularin-treated cells (Fig. 2F–G). These results indicated that Sinularin induces autophagy through inhibition of the mTOR pathway in prostate cancer cells.

Original blots are presented in Supplementary Fig. 2. The data are expressed as the mean \pm SD from three independent experiments. *** $P < 0.001$.

FOXO3 protein is involved in Sinularin induced autophagy

FOXO3 is a crucial tumor suppressor involved in a variety of cellular processes, including cell apoptosis, cell cycle progression, oxidative stress, and autophagy²⁶. Our previous study revealed that Sinularin stabilized FOXO3 protein in prostate cancer cells¹⁸. In this study, we further investigated whether FOXO3 protein is involved in Sinularin induced autophagy. As shown in Fig. 3A, the knockdown of FOXO3 expression inhibited LC3-II processing and blunted p62 degradation in Sinularin-treated LNCaP and PC-3 cells. Meanwhile, Sinularin-induced LC3-containing autophagic puncta were significantly decreased in FOXO3 knockdown PC-3 cells (Fig. 3B). These results indicated that the FOXO3 protein is involved in Sinularin induced autophagy.

Original blots are presented in Supplementary Fig. 3. The data are expressed as the mean \pm SD from three independent experiments. *** $P < 0.001$.

FOXO3 binds to the ATG4A promoter and regulates ATG4A expression

As FOXO3 is a key transcriptional factor, we searched for the target genes of FOXO3 protein. Our in-silicon search by JASPAR²⁷ predicted that the ATG4A gene is a downstream target of the FOXO3 since there are several potential binding sites in the ATG4A promoter region (Fig. 4A). Transient overexpression of FOXO3 up-regulated ATG4A expression at both the protein and mRNA levels (Fig. 4B). Promoter analysis using a dual-luciferase reporter system indicated that FOXO3 interacted with the ATG4A promoter at the -760 ~ -400 (-680 ~ -673) region (Fig. 4C–D). Mutating this region (-680 ~ -673) abolished FOXO3-induced reporter activity (Fig. 4E). These results indicated that the ATG4A gene is a FOXO3 downstream target.

Original blots are presented in Supplementary Fig. 4. The data are expressed as the mean \pm SD from three independent experiments. *** $P < 0.001$.

The FOXO3-ATG4A axis is up-regulated after Sinularin treatment

The cysteine protease ATG4A has been shown as an essential component in the formation and regulation of autophagosome membranes²⁸. In this study, we further investigated whether Sinularin treatment enhanced

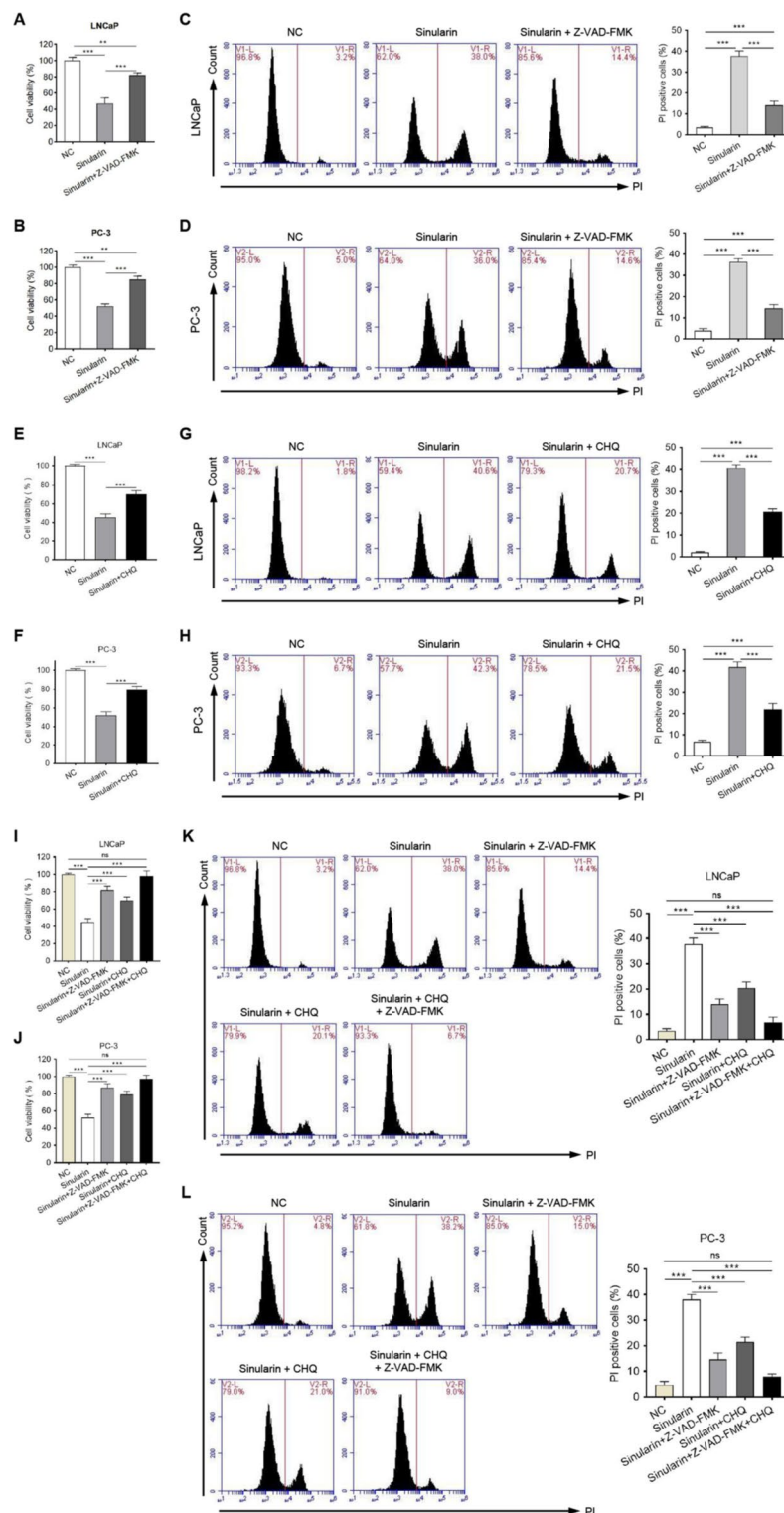


Fig. 1. Inhibition of autophagy and apoptosis blocks prostate cancer cell death caused by Sinularin. (A,B) Sinularin reduced the viability of LNCaP and PC-3 cells through apoptosis. (C,D) Sinularin induced cell death was decreased markedly when apoptosis was inhibited. (E,F) Sinularin reduced the viability of tumor cells through autophagy. (G,H) Sinularin induced autophagy-dependent cell death in prostate cancer cells. (I,J) Sinularin reduced the viability of prostate cancer cells through apoptosis and autophagy. (K,L) Inhibition of apoptosis and autophagy reversed Sinularin-induced cell death in prostate cancer cells. The data are expressed as the mean \pm SD from three independent experiments. *** $P < 0.001$.

ATG4A expression in PCa cells. As shown in Fig. 5A–B, our results showed that Sinularin up-regulated both ATG4A protein and mRNA expression in a dose-dependent manner. In addition, as expected, FOXO3 gene knockdown significantly reduced ATG4A expression in Sinularin-treated prostate cancer cells (Fig. 5C–D). These results indicated that up-regulation of the FOXO3–ATG4A axis is involved in Sinularin-treated prostate cancer cells.

Original blots are presented in Supplementary Fig. 5. The data are expressed as the mean \pm SD from three independent experiments. *** $P < 0.001$.

ATG4A protein is involved in Sinularin induced autophagy

We then determined whether ATG4A was involved in Sinularin-induced autophagy in prostate cancer cells. ATG4A gene was silenced through RNAi to decrease the expression of ATG4A protein (Fig. 6A). In ATG4A-knockdown cells, the number of autophagic puncta was significantly decreased (Fig. 6B). In addition, Sinularin-induced LC3 processing and p62 degradation were also attenuated when ATG4A gene expression was knocked down (Fig. 6C). These results indicated that ATG4A protein is involved in Sinularin induced autophagy.

Original blots are presented in Supplementary Fig. 6. The data are expressed as the mean \pm SD from three independent experiments. *** $P < 0.001$.

Sinularin-induced prostate cancer cell apoptosis depends on autophagy-mediated survivin degradation partially

We previously reported that Sinularin induced apoptotic cell death in prostate cancer cells¹⁸. Herein, we revealed that Sinularin also induced autophagy in prostate cancer cells. It has been reported that autophagy is cross-talking with the apoptosis pathway^{29,30}, we then asked if inhibition of apoptosis alters Sinularin-induced autophagy. Our results showed that the pan-caspase inhibitor Z-VAD-FMK had no significant effect on LC-3 processing and p62 protein degradation (Fig. 7A). We then asked if inhibition of autophagy altered Sinularin-induced apoptosis. As shown in Fig. 7B, CHQ pre-treatment largely reduced Sinularin-induced caspase-3 and PARP cleavage, two hallmarks of cell apoptosis. In addition, inhibition of autophagy dramatically reduced apoptotic cell death induced by Sinularin (Fig. 7C).

The anti-apoptotic protein survivin is an endogenous caspase inhibitor, preventing the processing of initiator caspase-9 and other effector caspases^{31,32}. It has been postulated that survivin was regulated by autophagy pathways³³. Therefore, we analyzed survivin expression in prostate cancer cells after Sinularin treatment. Our results showed that Sinularin drastically reduced survivin levels in a concentration-dependent manner (Fig. 7D). As expected, CHQ rescued survivin level completely (Fig. 7E). These results indicated that Sinularin stimulates survivin degradation via autophagy. We then determined whether Sinularin induced apoptosis through autophagic degradation of survivin protein in prostate cancer cells. As shown in Fig. 7F and G, survivin overexpression attenuated cell apoptosis induced by Sinularin. This data and our previous report suggested that Sinularin induced prostate cancer cell apoptosis partially through autophagy-mediated survivin degradation.

Original blots are presented in Supplementary Fig. 7. The data are expressed as the mean \pm SD from three independent experiments. *** $P < 0.001$.

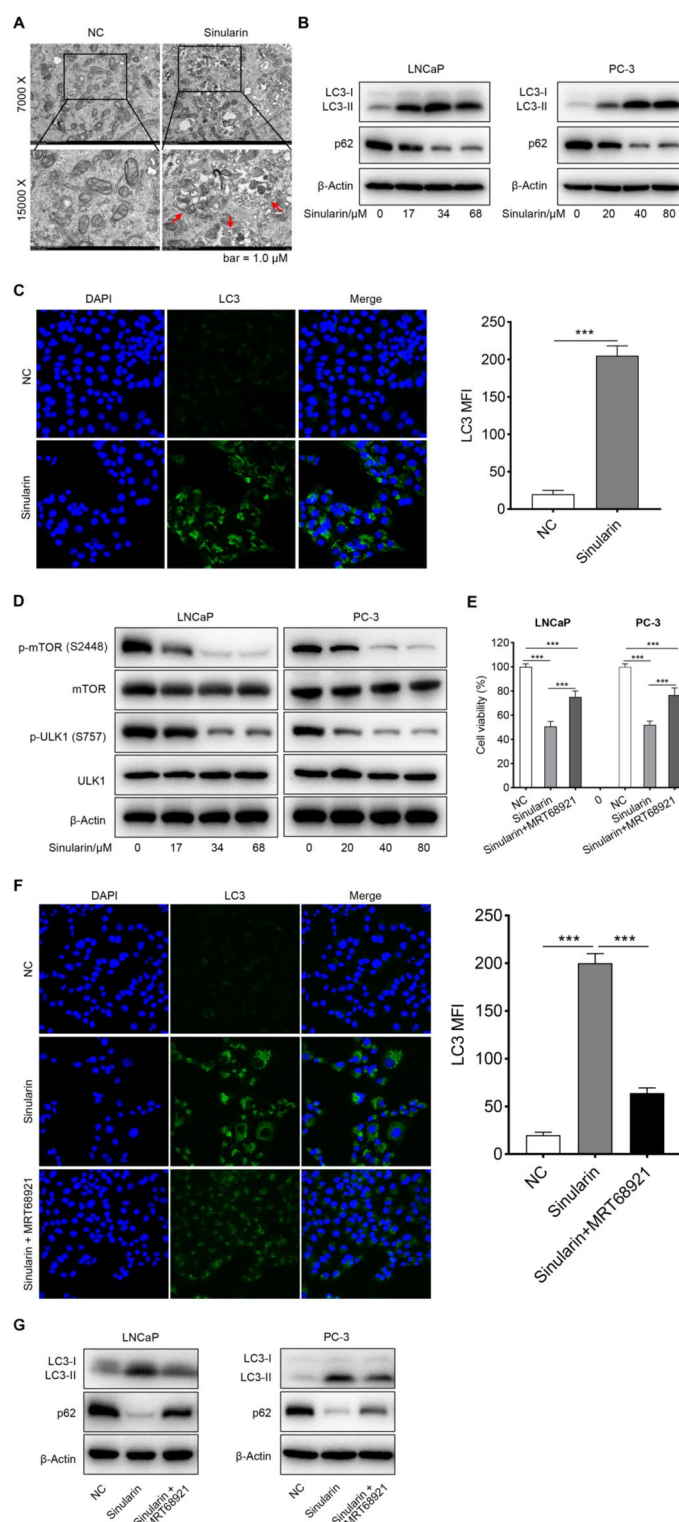
Discussion

Sinularin was reported to have anti-cancer effects in multiple cancers^{7–17}. We also demonstrated that Sinularin induced intrinsic apoptosis by stabilizing the FOXO3 protein in prostate cancer cells¹⁸. In this study, we further reported that Sinularin also promotes cell death of prostate cancer cells by autophagy.

Autophagy, an evolutionarily conserved catabolic process in which cells package bulk cytoplasmic contents, abnormal protein aggregates, and excess or damaged organelles through intracellular membrane structures to lysosomes for degradation, is critical for maintaining intracellular homeostasis³⁴. Generally, autophagy is a cellular strategy and mechanism for survival under stress. However, upon dysregulation of autophagy under certain circumstances, autophagy results in cell death, also known as type II programmed cell death³⁵. Autophagy is associated with multiple physiological and pathological processes such as development, differentiation, neurodegenerative diseases, stress, infection, and cancer³⁶. To date, the dual roles of autophagy in cancer progression and suppression remain controversial³⁷.

Autophagy is a multi-step process and is executed by numerous autophagy-related genes (ATG) and their core complexes³⁵. Unc-51-like kinase 1 (ULK1), a serine/threonine kinase, forms a large complex with ATG13 and FIP200 to initiate autophagy³⁸. In the study, we revealed that Sinularin activated ULK1 via reducing the phosphorylation at S757 site, and inhibition of ULK1 by MRT68921 largely reduced autophagy in Sinularin treated cells. The serine/threonine protein kinase mTOR (mammalian target of rapamycin) is a critical regulator of autophagy. Activation of mTOR suppressed autophagy by phosphorylation of ULK1 at Ser757 and prevention of ULK1 activation³⁹. A series of conditions can activate mTOR through PI3K/AKT and ERK/MAPK signaling or suppress mTOR via the AMPK pathway⁴⁰. Our previous study revealed that Sinularin significantly inhibited AKT and ERK1/2 phosphorylation¹⁸, as expected, as a downstream molecule of both of them, phosphorylation of mTOR is inhibited by Sinularin treatment (Fig. 2D). Thus, Sinularin promotes ULK1 activation and autophagy initiation by inhibition of the mTOR pathway in prostate cancer cells.

FOXO3 plays an essential role in mediating a variety of cellular processes, including apoptosis and autophagy²⁶. In our previous study, we demonstrated that Sinularin stabilized FOXO3 protein and promoted intrinsic apoptosis¹⁸. In the study, we demonstrated that Sinularin also induced autophagy through a dependent mechanism. In addition, we identified the ATG4A gene as a new target gene of FOXO3, its binding sites in the ATG4A promoter region at -680 ~ -673. ATG4A is a cysteine protease, which is essential for the formation and regulation of autophagosomes²⁸. ATG4A cleaves LC3 at its C-terminus to generate cytosolic LC3-I, which is subsequently conjugated to phosphatidylethanolamine and attached to the autophagosome membrane^{35,41}.



In the study, we demonstrated that Sinularin upregulated ATG4A expression through a FOXO3-dependent mechanism and ATG4A protein involved in Sinularin induced autophagy. These results revealed the key role of the FOXO3-ATG4A axis in Sinularin induced autophagy.

Previous studies showed an overlap mechanism between apoptosis and autophagy^{29,30}. Several pro-apoptotic signals, such as TNF, TRAIL, and FADD, also induce autophagy. Bcl-2, a critical anti-apoptotic factor, inhibits Beclin-1-dependent autophagy, thereby functioning as an anti-autophagic agent⁴². In this study, we demonstrated that inhibition of autophagy reduced Sinularin-induced apoptosis, indicating a pro-apoptotic role of Sinularin induced autophagy. Further analysis revealed that survivin, an anti-apoptotic protein, was significantly decreased after Sinularin treatment, and its level was rescued after inhibition of autophagy. These results suggested that Sinularin promoted survivin degradation through autophagy.

◀ **Fig. 2.** Sinularin induced autophagy through activating ULK1 in prostate cancer cells. **(A)** Transmission electron micrographs (TEM) showing autophagic vacuoles in PC-3 cells cultured with Sinularin for 24 h. Arrows indicate autophagosome structures. **(B)** Western blot analysis of the LC3 I/II and p62 levels in LNCaP and PC-3 cells treated with Sinularin for 24 h. **(C)** Representative immunofluorescence images and mean fluorescence intensity (MFI) quantification of LC3 taken from PC-3 cells treated with Sinularin for 24 h. Autophagosomes were visualized and examined via immunofluorescence microscopy through photographs of LC3 puncta. **(D)** Western blot analysis was used to determine the phosphorylation levels of mTOR (Ser 2448) and ULK1 (Ser 757) in LNCaP and PC-3 cells treated with Sinularin for 24 h. **(E)** The cell viability was measured by MTS assay in LNCaP and PC-3 cells treated with Sinularin alone or in combination with ULK1 inhibitor MRT68921. **(F)** Representative immunofluorescence images and mean fluorescence intensity (MFI) quantification of LC3 taken from PC-3 cells treated with Sinularin alone or in combination with ULK1 inhibitor MRT68921. Autophagosomes were visualized and examined via immunofluorescence microscopy through photographs of LC3 puncta. **(G)** Western blot analysis of LC3 I/II and p62 levels in LNCaP and PC-3 cells treated with Sinularin alone or in combination with the ULK1 inhibitor MRT68921.

In the study, we demonstrated that inhibiting ferroptosis pathway by both ferroptosis inhibitors ferrostatin-1 (Fer-1) and deferoxamine mesylate (DFOM), had no significant effect on Sinularin induced cell death. However, a recent study by Wu et al. suggested that Sinularin induced ferroptosis in prostate cancer cells⁴³. The differences may cause by longer treated time and lower Sinularin concentration. In addition, the different results showed the complicated and interesting mechanisms under Sinularin induced cell death, which prompted the further study of us.

In conclusion, Sinularin induced autophagy in prostate cancer cells by activation of ULK1 to trigger autophagy initiation through the mTOR pathway and enhance of FOXO3-ATG4A axis to promote vesicle elongation and autophagosome completion. Furthermore, Sinularin induced autophagy-dependent survivin degradation, which in turn promoted cell apoptosis (Fig. 8). Therefore, our findings provided a novel insight into the mechanism underlying Sinularin-induced cell death.

Sinularin induced prostate cancer cell autophagy through activating ULK1 via mTOR inhibition to trigger autophagy induction, and promoting the autophagic protein ATG4A expression through a FOXO3-dependent transcriptional mechanism. Furthermore, Sinularin induced autophagy resulted in survivin degradation, leading to cell apoptosis. We previously also reported that FOXO3 upregulates PUMA and promotes intrinsic apoptosis in prostate cancer cells. Taken together, these findings revealed complicated mechanisms involved in Sinularin-induced prostate cancer cell death.

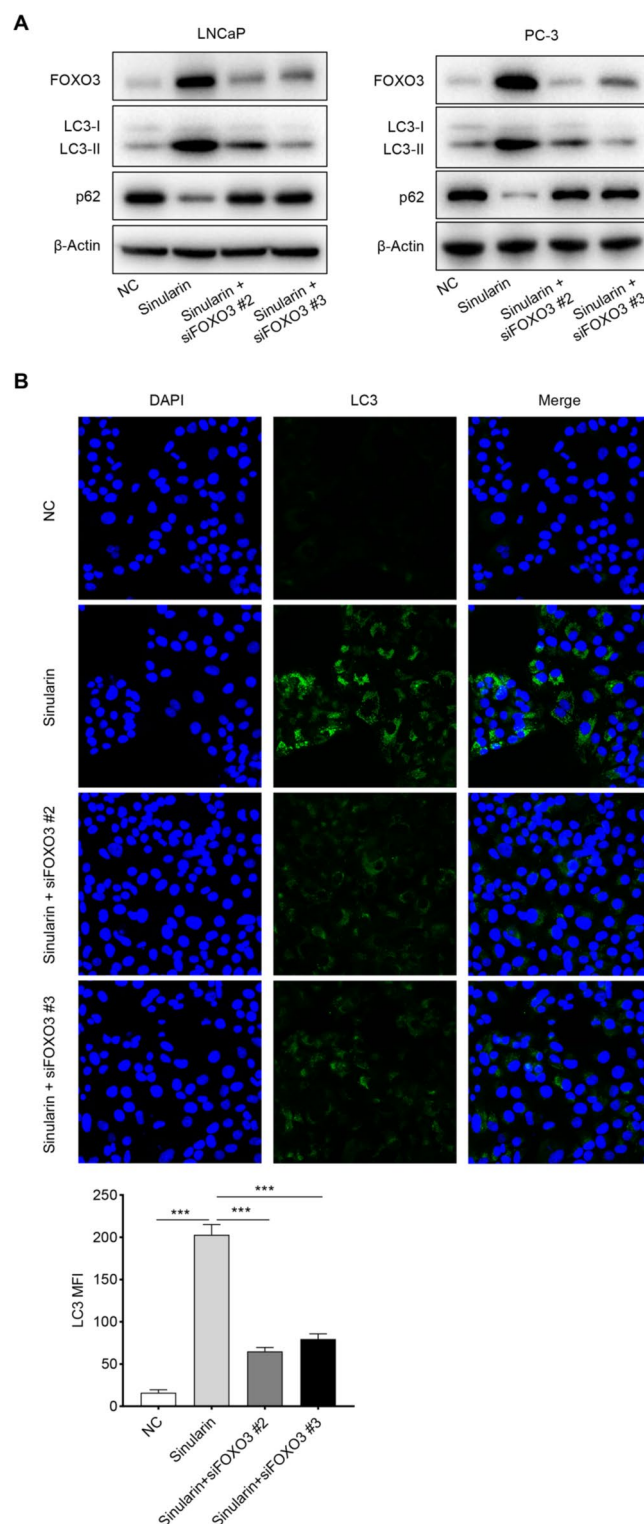


Fig. 3. Sinularin induced autophagy via FOXO3. **(A)** Western blot analysis to determine the LC3 I/II and p62 levels in Sinularin-treated LNCaP and PC-3 cells following FOXO3 knockdown. **(B)** Representative immunofluorescence images and mean fluorescence intensity (MFI) quantification of LC3 taken from PC-3 cells treated with Sinularin or subjected to FOXO3 knockdown. Autophagosomes were visualized and examined via immunofluorescence microscopy through photographs of LC3 puncta.

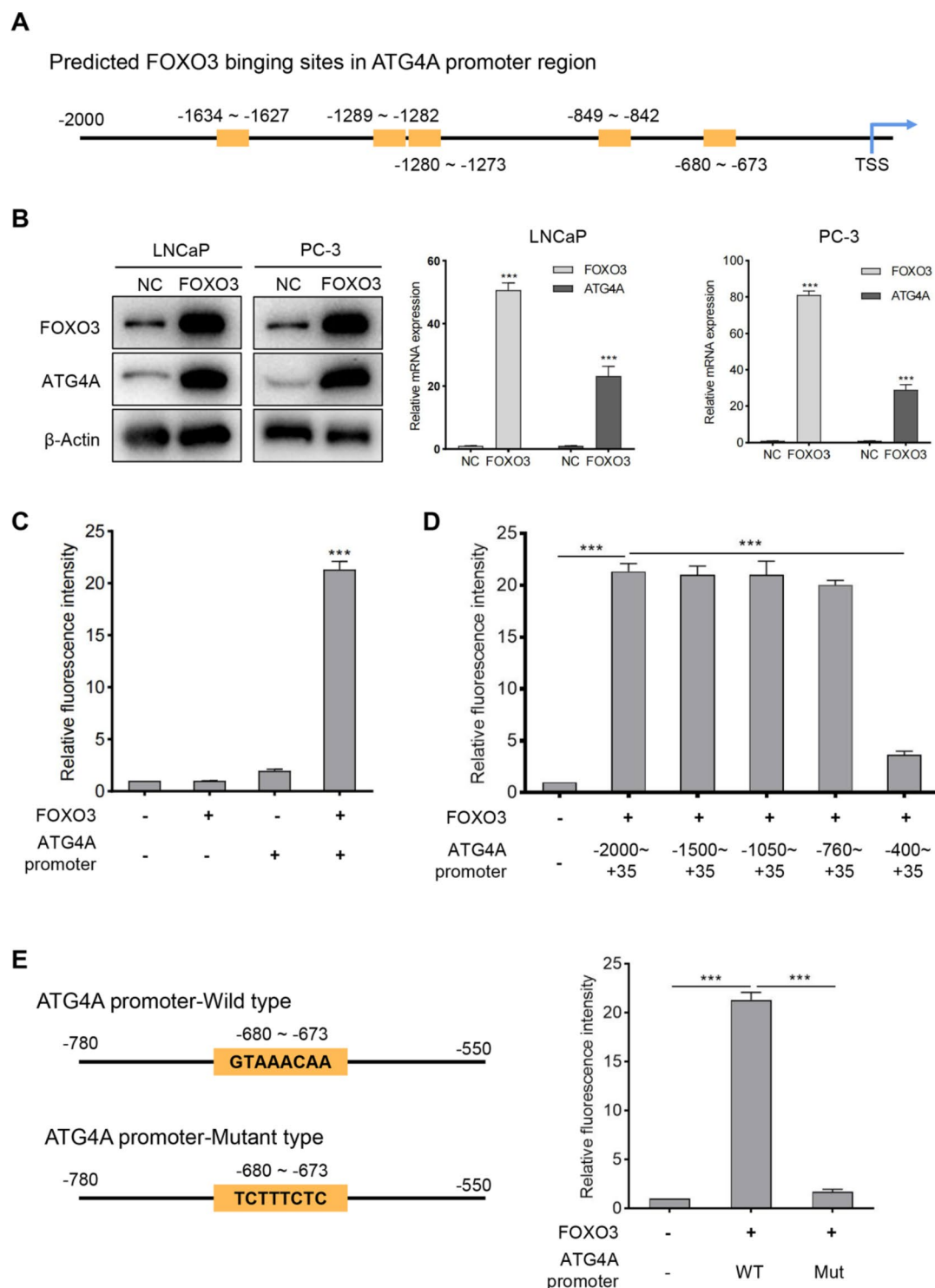


Fig. 4. FOXO3 binds to the ATG4A promoter and regulates ATG4A expression. **(A)** Bioinformatic algorithms predicted that ATG4A is a target gene of the transcription factor FOXO3 and that there are several possible binding sites in the ATG4A promoter region. **(B)** After overexpressing FOXO3 in LNCaP and PC-3 cells, the protein and mRNA expression of ATG4A was measured by western blot and qRT-PCR, respectively. **(C)** 293T cells were co-transfected with the luciferase reporter vector containing the ATG4A promoter and the FOXO3 overexpression vector. Then, the luciferase density was measured. **(D)** 293T cells were co-transfected with the luciferase reporter vector containing the truncated ATG4A promoter and the FOXO3 overexpression vector. Then, the luciferase density was measured. **(E)** Luciferase reporter vector containing the ATG4A promoter sequence, the wild type (WT) or the corresponding mutant (MUT), was co-transfected with the FOXO3 overexpression vector in 293T cells. Then, the luciferase density was measured.

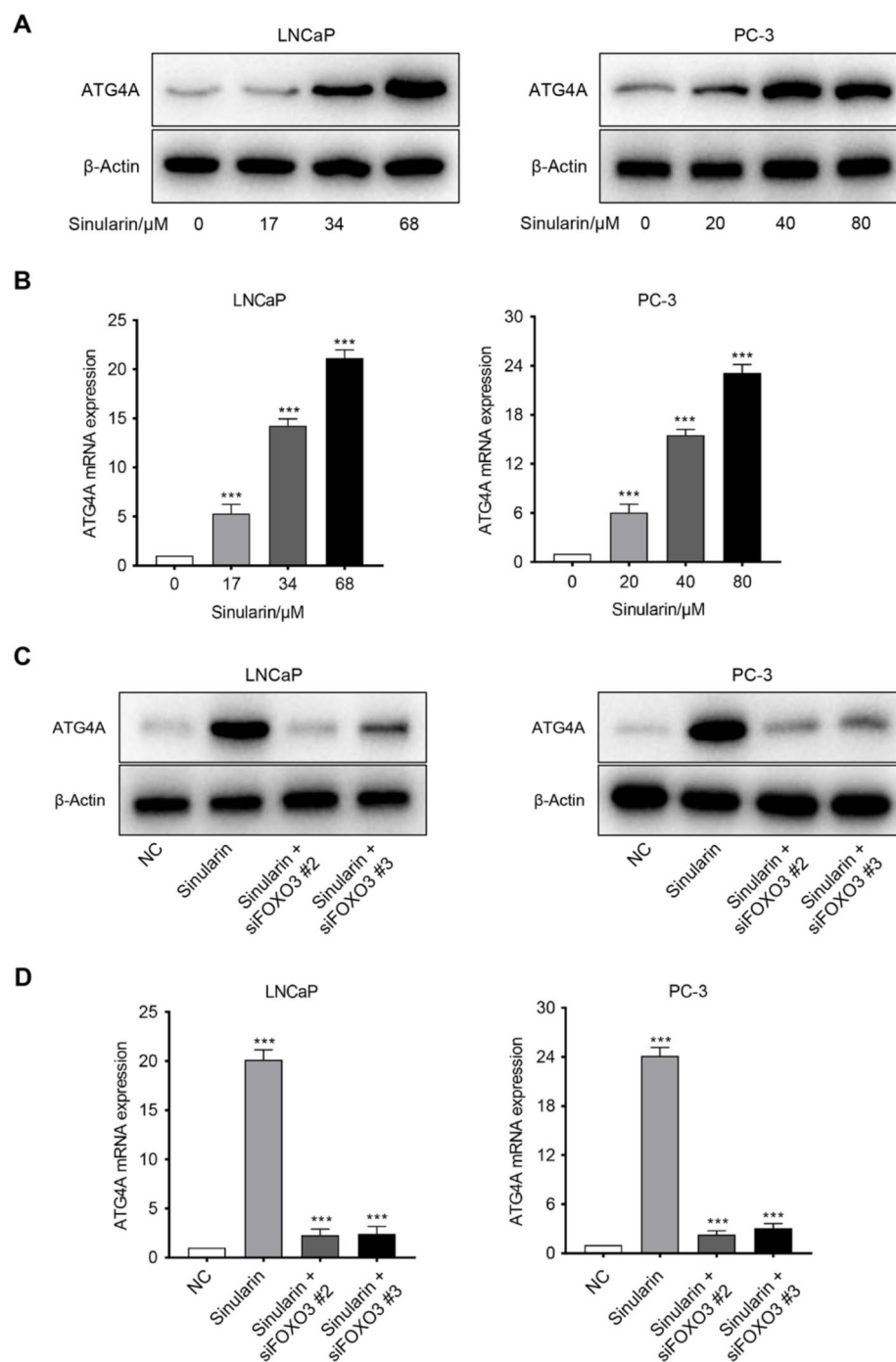


Fig. 5. The FOXO3-ATG4A axis is regulated by Sinularin in prostate cancer cells. (**A,B**) Western blot and qRT-PCR analyses were performed to determine the protein and mRNA expression levels of ATG4A in LNCaP and PC-3 cells treated with Sinularin for 24 h. (**C,D**) After FOXO3 was knocked down in Sinularin-treated LNCaP and PC-3 cells, the protein and mRNA expression of ATG4A was measured by western blot and qRT-PCR, respectively.

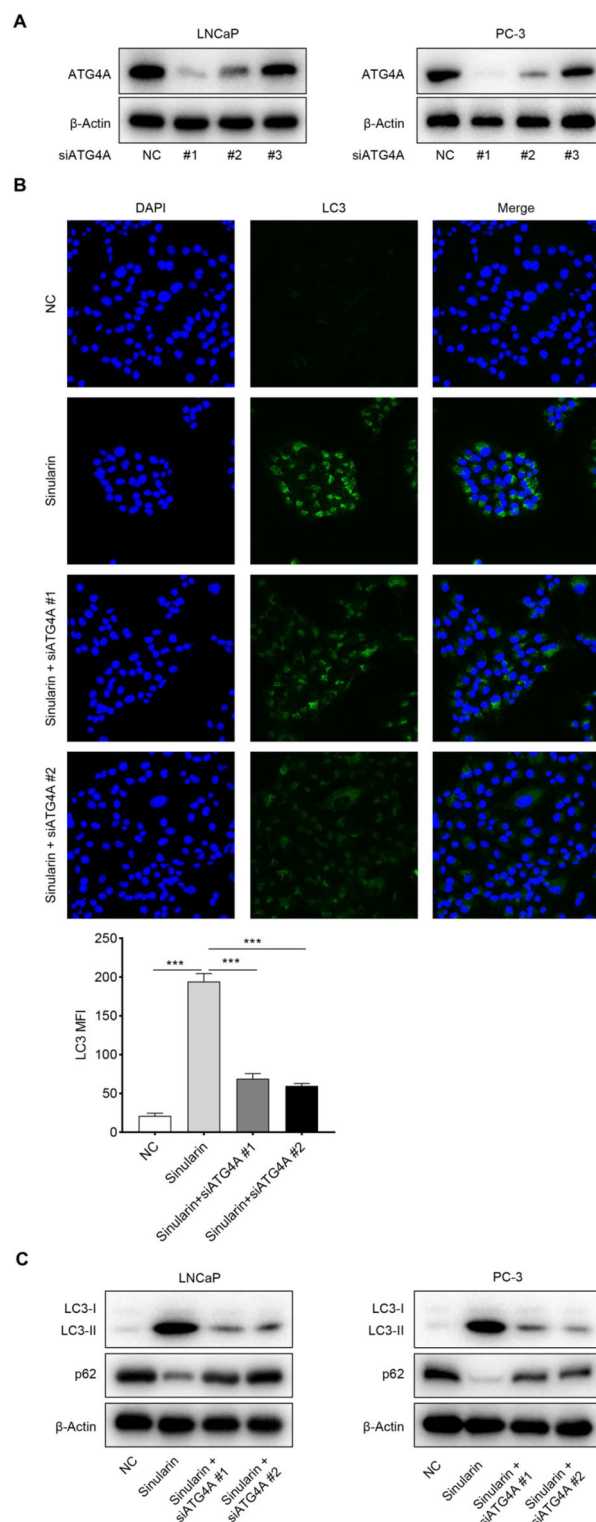


Fig. 6. Sinularin induces prostate cancer cell autophagy through ATG4A. (A) Western blot analysis was used to determine ATG4A protein expression after ATG4A was knocked down by siRNAs. (B) Representative immunofluorescence images and mean fluorescence intensity (MFI) quantification of LC3 taken from PC-3 cells treated with Sinularin or subjected to ATG4A knockdown. Autophagosomes were visualized and examined via immunofluorescence microscopy through photographs of LC3 puncta. (C) Western blot analysis to determine the LC3 I/II and p62 levels in Sinularin-treated LNCaP and PC-3 cells following ATG4A knockdown.

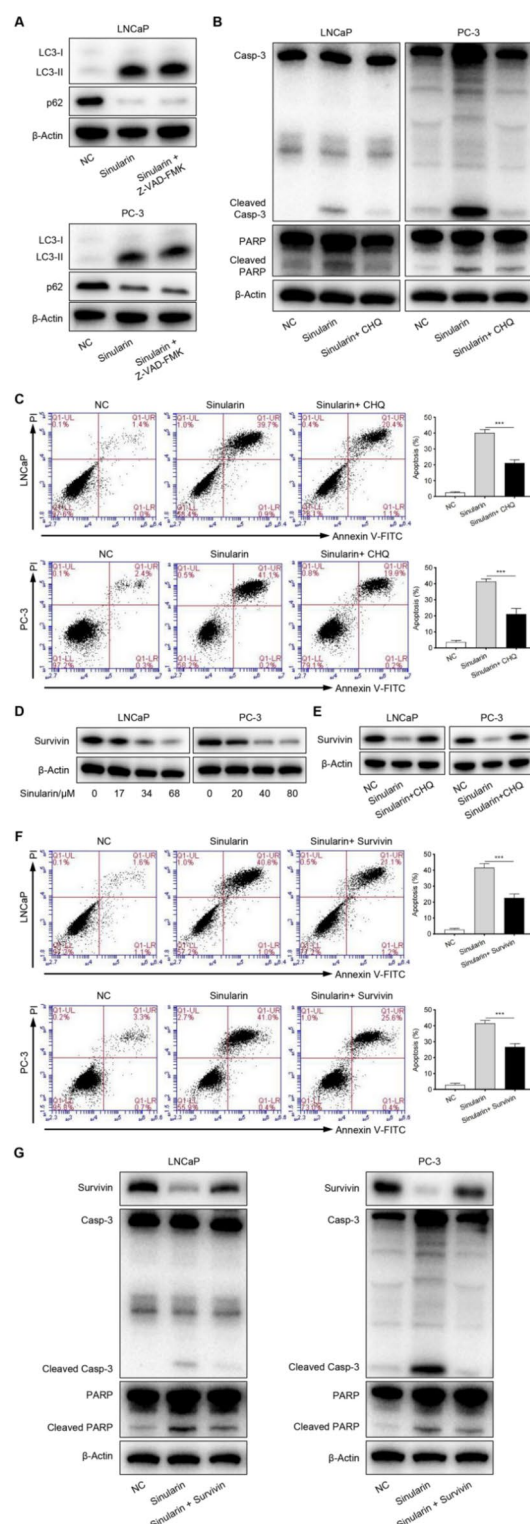


Fig. 7. Sinularin induced prostate cancer cell apoptosis through autophagic degradation of survivin protein. **(A)** After apoptosis was inhibited by Z-VAD-FMK, the LC3 I/II, and p62 protein levels were determined via western blot analysis in Sinularin-treated LNCaP and PC-3 cells. **(B)** Western blot analysis of cleaved PARP and cleaved caspase 3 in Sinularin-treated LNCaP and PC-3 cells following the inhibition of autophagy by chloroquine (CHQ). **(C)** After autophagy was inhibited by chloroquine (CHQ), cell apoptosis was measured via flow cytometry (FCM) analysis in Sinularin-treated LNCaP and PC-3 cells. **(D)** Western blot analysis of survivin protein levels in Sinularin-treated LNCaP and PC-3 cells. **(E)** After autophagy was inhibited by chloroquine (CHQ), survivin protein level in Sinularin-treated LNCaP and PC-3 cells was determined by western blot analysis. **(F)** Cell apoptosis was measured by flow cytometry (FCM) analysis in Sinularin-treated LNCaP and PC-3 cells following the upregulation of survivin. **(G)** Western blot analysis of cleaved PARP and cleaved caspase 3 in Sinularin-treated LNCaP and PC-3 cells following the upregulation of survivin.

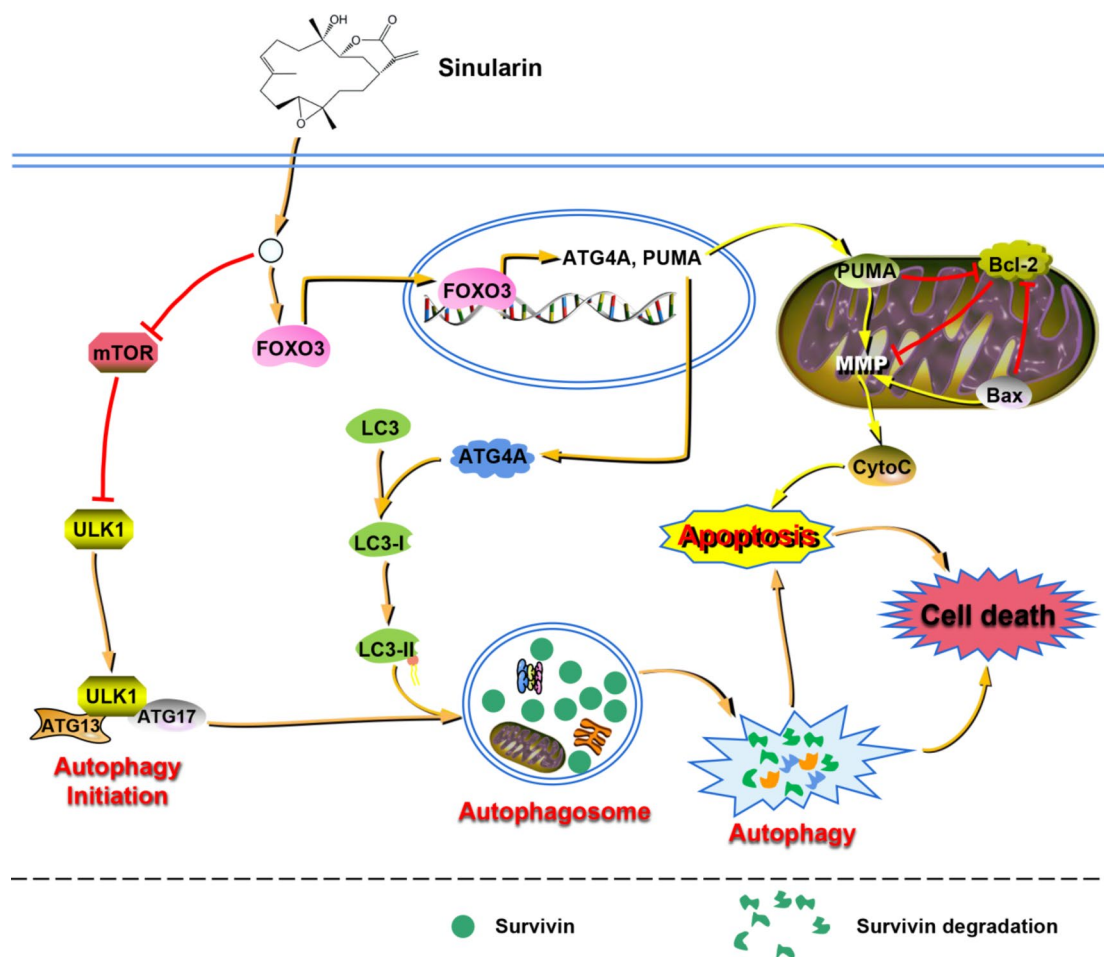


Fig. 8. Sinularin induces autophagy and apoptosis in prostate cancer cells.

Data availability

Data is provided within the manuscript or supplementary information files.

Received: 4 February 2025; Accepted: 2 May 2025

Published online: 07 May 2025

References

- Wu, L., Ye, K., Jiang, S. & Zhou, G. Marine power on cancer: drugs, lead compounds, and mechanisms. *Mar. Drugs* **19** (9), 488 (2021).
- Jimenez, P. C. et al. Enriching cancer Pharmacology with drugs of marine origin. *Br. J. Pharmacol.* **177** (1), 3–27 (2020).
- Blair, H. A. Daunorubicin/Cytarabine liposome: A review in acute myeloid leukaemia. *Drugs* **78** (18), 1903–1910 (2018).
- Levy, J. H., Ghadimi, K., Kizhakkedathu, J. N. & Iba, T. What's fishy about Protamine?? Clinical use, adverse reactions, and potential alternatives. *J. Thromb. Haemost.* **21** (7), 1714–1723 (2023).
- Seifert, R. Vidarabine is neither a potent nor a selective AC5 inhibitor. *Biochem. Pharmacol.* **87** (4), 543–546 (2014).
- Saeed, A. F. U. H., Su, J. & Ouyang, S. Marine-derived drugs: recent advances in cancer therapy and immune signaling. *Biomed. Pharmacother.* **134**, 111091 (2021).
- Su, T. R. et al. Proteomic investigation of anti-tumor activities exerted by sinularin against A2058 melanoma cells. *Electrophoresis* **33** (7), 1139–1152 (2012).
- Wu, Y. J., Wong, B. S., Yea, S. H., Lu, C. I. & Weng, S. H. Sinularin induces apoptosis through mitochondria dysfunction and inactivation of the p13K/Akt/mTOR pathway in gastric carcinoma cells. *Mar. Drugs* **14** (8), 142 (2016).
- Chang, Y. T. et al. Sinularin induces oxidative stress-mediated G2/M arrest and apoptosis in oral cancer cells. *Environ. Toxicol.* **32** (9), 2124–2132 (2017).
- Peng, S. Y. et al. Oxidative Stress-Dependent synergistic antiproliferation, apoptosis, and DNA damage of Ultraviolet-C and Coral-Derived sinularin combined treatment for oral Cancer cells. *Cancers (Basel)* **13** (10), 2450 (2021).
- Yang, K. H. et al. Soft Coral-Derived Dihydrosinularin exhibits antiproliferative effects associated with apoptosis and DNA damage in oral Cancer cells. *Pharmaceuticals (Basel)* **14** (10), 994 (2021).
- Ko, C. Y. et al. Sinularin, an Anti-Cancer agent causing Mitochondria-Modulated apoptosis and cytoskeleton disruption in human hepatocellular carcinoma. *Int. J. Mol. Sci.* **22** (8), 3946 (2021).
- Chung, T. W. et al. Sinularin induces DNA damage, G2/M phase arrest, and apoptosis in human hepatocellular carcinoma cells. *BMC Complement. Altern. Med.* **17** (1), 62 (2017).
- Huang, H. W. et al. Sinularin selectively kills breast Cancer cells showing G2/M arrest, apoptosis, and oxidative DNA damage. *Molecules* **23** (4), 849 (2018).

15. Hossain, R. et al. Natural compounds or their derivatives against breast cancer: A computational study. *Biomed. Res. Int.* **2022**, 5886269 (2022).
16. Wang, S. C. et al. Comparison of antioxidant and anticancer properties of soft Coral-Derived sinularin and Dihydrosinularin. *Molecules* **26** (13), 3853 (2021).
17. Ma, Q. et al. Sinularin exerts anti-tumor effects against human renal cancer cells relies on the generation of ROS. *J. Cancer*. **10** (21), 5114–5123 (2019).
18. Meng, X. Y. et al. Sinularin stabilizes FOXO3 protein to trigger prostate cancer cell intrinsic apoptosis. *Biochem. Pharmacol.* **220**, 116011 (2024).
19. Meng, X. Y. et al. Pinin promotes tumor progression via activating CREB through PI3K/AKT and ERK/MAPK pathway in prostate cancer. *Am. J. Cancer Res.* **11** (4), 1286–1303 (2021).
20. Meng, X. et al. MiR-125b-2-3p associates with prognosis of CcRCC through promoting tumor metastasis via targeting EGR1. *Am. J. Transl. Res.* **12** (9), 5575–5585 (2020).
21. Ma, L. et al. Rhein promotes TRAIL-induced apoptosis in bladder cancer cells by up-regulating DR5 expression. *Aging (Albany NY)*. **14** (16), 6642–6655 (2022).
22. Wang, X. et al. Decrease of phosphorylated proto-oncogene CREB at Ser 133 site inhibits growth and metastatic activity of renal cell cancer. *Expert Opin. Ther. Targets*. **19** (7), 985–995 (2015).
23. Lei, G., Zhuang, L. & Gan, B. Targeting ferroptosis as a vulnerability in cancer. *Nat. Rev. Cancer*. **22** (7), 381–396 (2022).
24. Panwar, V. et al. Multifaceted role of mTOR (mammalian target of rapamycin) signaling pathway in human health and disease. *Signal. Transduct. Target. Ther.* **8** (1), 375 (2023).
25. Kim, J., Kundu, M., Viollet, B. & Guan, K. L. AMPK and mTOR regulate autophagy through direct phosphorylation of Ulk1. *Nat. Cell. Biol.* **13** (2), 132–141 (2011).
26. Calissi, G., Lam, E. W. & Link, W. Therapeutic strategies targeting FOXO transcription factors. *Nat. Rev. Drug Discov.* **20** (1), 21–38 (2021).
27. Fornes, O. et al. JASPAR 2020: update of the open-access database of transcription factor binding profiles. *Nucleic Acids Res.* **48** (D1), D87–D92 (2020).
28. Stolla, M. C. et al. ATG4A regulates human erythroid maturation and mitochondrial clearance. *Blood Adv.* **6** (12), 3579–3589 (2022).
29. Soric, M. Crosstalk of autophagy and apoptosis. *Cells* **11** (9), 1479 (2022).
30. Das, S., Shukla, N., Singh, S. S., Kushwaha, S. & Shrivastava, R. Mechanism of interaction between autophagy and apoptosis in cancer. *Apoptosis* **26** (9–10), 512–533 (2021).
31. Zafari, P., Rafiei, A., Esmaili, S. A., Moonesi, M. & Taghadossi, M. Survivin a pivotal antiapoptotic protein in rheumatoid arthritis. *J. Cell. Physiol.* **234** (12), 21575–21587 (2019).
32. Martínez-García, D., Manero-Rupérez, N., Quesada, R., Korrodi-Gregório, L. & Soto-Cerrato, V. Therapeutic strategies involving survivin Inhibition in cancer. *Med. Res. Rev.* **39** (3), 887–909 (2019).
33. Gorski, S. M. et al. A SAGE approach to discovery of genes involved in autophagic cell death. *Curr. Biol.* **13** (4), 358–363 (2003).
34. Mizushima, N. & Komatsu, M. Autophagy: renovation of cells and tissues. *Cell* **147** (4), 728–741 (2011).
35. Levine, B. & Kroemer, G. Biological functions of autophagy genes: A disease perspective. *Cell* **176** (1–2), 11–42 (2019).
36. Kim, K. H. & Lee, M. S. Autophagy—a key player in cellular and body metabolism. *Nat. Rev. Endocrinol.* **10** (6), 322–337 (2014).
37. Levy, J. M. M., Towers, C. G. & Thorburn, A. Targeting autophagy in cancer. *Nat. Rev. Cancer*. **17** (9), 528–542 (2017).
38. Zachari, M. & Ganley, I. G. The mammalian ULK1 complex and autophagy initiation. *Essays Biochem.* **61** (6), 585–596 (2017).
39. Kim, Y. C. & Guan, K. L. mTOR: a Pharmacologic target for autophagy regulation. *J. Clin. Invest.* **125** (1), 25–32 (2015).
40. Liu, G. Y. & Sabatini, D. M. mTOR at the nexus of nutrition, growth, ageing and disease. *Nat. Rev. Mol. Cell. Biol.* **21** (4), 183–203 (2020).
41. Nguyen, T. N. et al. ATG4 family proteins drive phagophore growth independently of the LC3/GABARAP lipidation system. *Mol. Cell.* **81** (9), 2013–2030e9 (2021).
42. Su, Z., Yang, Z., Xu, Y., Chen, Y. & Yu, Q. Apoptosis, autophagy, necroptosis, and cancer metastasis. *Mol. Cancer*. **14**, 48 (2015).
43. Wu, Z. et al. Sinularin exerts Anti-cancer effects by inducing oxidative Stress-mediated ferroptosis, apoptosis, and autophagy in prostate Cancer cells. *Anticancer Agents Med. Chem.* **23** (12), 1457–1468 (2023).

Author contributions

XY. M. and Q. M. conceived the study; XY. M., R. Y., ZJ. Y. and Q. M. designed the experiments; XY. M., Y. L., SZ. Y., KJ. W. and JF. C. performed the experiments and wrote the manuscript; XY. M., Y. L. and SZ. Y. conducted data analysis. All authors have read and approved the manuscript.

Funding

This work was supported by Natural Science Foundation of Ningbo (2021J259 and 2024J343 to Xiang-yu Meng, 20221JCGY010080 to Sha-zhou Ye and 2023J158 to Ke-jie Wang), Natural Science Foundation of Zhejiang Province (LQ20H160008 to Jun-feng Chen), Medical and Health Science and Technology Program of Zhejiang Province (2023KY258 to Jun-feng Chen), Ningbo Medical Science and Technology Project (2021Y06 to Sha-zhou Ye), Fund of Ningbo Clinical Research Center for Urological Disease (2019A21001), Ningbo Top Medical and Health Research Program (2022020203), and Zhejiang Engineering Research Center of Innovative technologies and diagnostic and therapeutic equipment for urinary system diseases.

Declarations

Competing interests

The authors declare no competing interests.

Consent for publication

All authors consent this manuscript for publication.

Additional information

Supplementary Information The online version contains supplementary material available at <https://doi.org/10.1038/s41598-025-00909-3>.

Correspondence and requests for materials should be addressed to R.Y. or Q.M.

Reprints and permissions information is available at www.nature.com/reprints.

Publisher's note Springer Nature remains neutral with regard to jurisdictional claims in published maps and institutional affiliations.

Open Access This article is licensed under a Creative Commons Attribution-NonCommercial-NoDerivatives 4.0 International License, which permits any non-commercial use, sharing, distribution and reproduction in any medium or format, as long as you give appropriate credit to the original author(s) and the source, provide a link to the Creative Commons licence, and indicate if you modified the licensed material. You do not have permission under this licence to share adapted material derived from this article or parts of it. The images or other third party material in this article are included in the article's Creative Commons licence, unless indicated otherwise in a credit line to the material. If material is not included in the article's Creative Commons licence and your intended use is not permitted by statutory regulation or exceeds the permitted use, you will need to obtain permission directly from the copyright holder. To view a copy of this licence, visit <http://creativecommons.org/licenses/by-nc-nd/4.0/>.

© The Author(s) 2025